

СИБИРСКИЕ ЭЛЕКТРОННЫЕ
МАТЕМАТИЧЕСКИЕ ИЗВЕСТИЯ

Siberian Electronic Mathematical Reports

<http://semr.math.nsc.ru>

Том 19, №2, стр. 517–527 (2022)
DOI 10.33048/semi.2022.19.043УДК 51-73
MSC 86-10RECONSTRUCTION OF SUBSURFACE SCATTERING OBJECTS
BY THE TIME REVERSAL MIRROR

G. RESHETOVA, A. GALAKTIONOVA

Recovery and spatial localization of small scale inhomogeneities in geological media are of fundamental importance to increase the resolution of the geophysical data processing and improve reliability of the results obtained. This paper proposes a method for reconstruction of random subseismic inhomogeneities embedded in a smooth elastic medium using the Time Reversal Mirror approach. The method is based on the time reversibility principle of wave processes in media without attenuation. The interaction of a wavefield with subseismic inhomogeneities is considered as the process of the appearance of "secondary sources" generated by small-scale inclusions. These sources indicate the presence of the geological inhomogeneities in a medium and can be spatially localized using the Time Reversal Mirror method based on the recordings of the data by the acquisition system. Verification of the method proposed was carried out on synthetic data computed by the finite difference method.

Keywords: random media, wave propagation, secondary radiation sources, numerical solutions, Time Reversal Mirror, finite difference schemes.

1. INTRODUCTION

The main goal of the exploration geophysics is to search for the structure of hydrocarbon and mineral deposits. One of the principal areas of geophysical research is seismic exploration on the basis of the excitation and recording of elastic waves. Different geological media have different elastic properties which gives rise of reflected/scattered waves at the interfaces of the layers. These waves bring information about geological structures. They can be recorded by seismic receivers and

RESHETOVA, G., GALAKTIONOVA, A., RECONSTRUCTION OF SUBSURFACE SCATTERING OBJECTS BY THE TIME REVERSAL MIRROR.

© 2022 RESHETOVA G., GALAKTIONOVA A.

Received May, 20, 2022, published August, 24, 2022.

subjected to special processing to restore the Earth's internal structure. For example, using the methods of reflected or refracted waves, the geometry of boundaries in layered media is restored with sufficient reliability. However, the identification of clusters of small-scale irregularities can cause serious difficulties. The characteristic sizes of these objects are much smaller than the dominant length of seismic waves and therefore cause an extremely weak response. However, the presence of small-scale inhomogeneities in the medium leads to the appearance of a field of scattered waves, which can be considered as indicator to the inhomogeneity of the geological medium. Therefore, if we localize the origin of a scattered wave, we thereby determine the position of the scatterer that has generated it. Thus, the problem of determining the location of small-scale inhomogeneities within a geological medium can be reduced to the problem of finding the position of sources of scattered waves generated by these inhomogeneities. Among the numerical methods and approaches for the localization of acoustic/seismic wave sources [1, 10], we have chosen the approach known as the Time Reversal Mirror (TRM) method.

The TRM method is based on the time reversibility property of the wave propagation in media without attenuation. Both the method and the term TRM were first introduced in [2]. In the last decade, this approach was very successfully used in solving problems of the virtual sources generation, sound focusing, non-destructive testing of materials and engineering structures, and in a number of other areas [3–6, 12].

One of the most important consequences of the time reversibility principle is the possibility of using inverted in time data recorded in receivers signal as source functions. With such an operation, the wavefield, by virtue of the principle formulated above, should be focused into the source both in space and in time and, thereby, generate the increase of the amplitude at the source point at the moment of its excitation.

However, in a number of practically significant cases, the moment of switching on the source is unknown; therefore, with the Time Reversal, the wave after the moment of focusing will inevitably to diverge and to lose the spatial localization. If there is a small number of sources (for example, less than ten), then such wave amplification can be visually followed, but if there are hundreds or more sources (in particular, during the destruction of the medium and the formation of a family of cracks), then visual tracking is no longer possible.

To overcome this problem we propose an original method for imaging the spatial localization of small-scale inhomogeneities based on the computation of the total energy of the time-reversal wavefield.

Below, we describe a scheme for solving the problem of localizing small-scale inhomogeneities within a smooth geological medium using a combination of the TRM for wavefield records on the free surface and the method for calculating the full elastic energy.

2. MODEL FORMULATION AND GOVERNING EQUATIONS

Let the half-plane $z \geq 0$ be filled with an elastic medium containing clusters of small-scale inhomogeneities. The propagation of elastic waves in such a medium satisfies the following system of the dynamic elasticity theory in the velocity-stress

formulation [11]:

$$(1) \quad \begin{cases} \rho \frac{\partial u_x}{\partial t} = \frac{\partial \tau_{xx}}{\partial x} + \frac{\partial \tau_{xz}}{\partial z} \\ \rho \frac{\partial u_z}{\partial t} = \frac{\partial \tau_{xz}}{\partial x} + \frac{\partial \tau_{zz}}{\partial z} \\ \frac{\partial \tau_{xx}}{\partial t} = (\lambda + 2\mu) \frac{\partial u_x}{\partial x} + \lambda \frac{\partial u_z}{\partial z} + F_{xx} \\ \frac{\partial \tau_{zz}}{\partial t} = (\lambda + 2\mu) \frac{\partial u_z}{\partial z} + \lambda \frac{\partial u_x}{\partial x} + F_{zz} \\ \frac{\partial \tau_{xz}}{\partial t} = \mu \left(\frac{\partial u_x}{\partial z} + \frac{\partial u_z}{\partial x} \right) + F_{xz} \end{cases}$$

In (1) the (v_x, v_z) are the displacement velocities, while $(\tau_{xx}, \tau_{xz}, \tau_{zz})$ correspond to stresses. The elastic parameters are the Lamé moduli λ, μ and the density ρ . There are the following connections of these parameters with P- and S-waves propagation velocities:

$$(2) \quad \lambda = \rho (V_p^2 - 2V_s^2), \quad \mu = \rho V_s^2.$$

The functions F_{xx}, F_{zz}, F_{xz} in the right-hand side of equations (1) define the seismic source. Here we deal with the volumetric source:

$$(3) \quad F_{xx} = F_{zz} = f(t) \cdot \delta(x - x_0, z - z_0), \quad F_{xz} = 0,$$

where $\delta(x - x_0, z - z_0)$ is the Dirac delta function centered at the point (x_0, z_0) , and $f(t)$ defines the source function, which chosen in our numerical experiments as the Ricker wavelet:

$$(4) \quad f(t) = (1 - 2\pi^2 f_0^2 (t - t_0)^2) \exp(-\pi^2 f_0^2 (t - t_0)^2),$$

with dominant frequency f_0 and time delay t_0 .

To avoid artificial reflections from the boundaries of the computational domain, we apply absorbing boundary conditions in the form of a perfectly matched layer (PML method). We use an unsplit convolutional PML [7], which has less spurious reflections than classical discrete PML.

3. LINEAR APPROXIMATION AND TOTAL ELASTIC ENERGY OF TRM

This section has two objectives. First, we justify that clusters of small-scale inhomogeneities can be considered as objects that generate secondary sources of scattered waves. Second, we outline an algorithm for localizing the accumulation of these inhomogeneities using the Time Reversal Mirror approach.

Since the inhomogeneities are assumed to be small compared to the wavelength, we can linearize equations (1). Let us represent the Lamé parameters of the medium in the form

$$(5) \quad \begin{aligned} \lambda(x, z) &= \lambda_0(x, z) + \lambda_1(x, z), \quad \lambda_1(x, z) \ll \lambda_0(x, z), \\ \mu(x, z) &= \mu_0(x, z) + \mu_1(x, z), \quad \mu_1(x, z) \ll \mu_0(x, z), \\ \rho(x, z) &= \rho_0(x, z) + \rho_1(x, z), \quad \rho_1(x, z) \ll \rho_0(x, z), \end{aligned}$$

where λ_0, μ_0, ρ_0 are parameters corresponding to smooth background, and the terms λ_1, μ_1, ρ_1 are sharp perturbations of the medium. Thus we represent the elastic parameters of the medium as the superposition of the two components - a smoothly varying macroscopic model (with index 0) and its small-scale perturbations (with

index 1). On the base of (5) we can also introduce the decomposition of the wavefield:

$$(6) \quad \begin{aligned} \vec{u}(x, z; t) &= \vec{u}_0(x, z; t) + \vec{u}_1(x, z; t), \\ \tau_{xx}(x, z; t) &= \tau_{xx}^0(x, z; t) + \tau_{xx}^1(x, z; t), \\ \tau_{zz}(x, z; t) &= \tau_{zz}^0(x, z; t) + \tau_{zz}^1(x, z; t), \\ \tau_{xz}(x, z; t) &= \tau_{xz}^0(x, z; t) + \tau_{xz}^1(x, z; t). \end{aligned}$$

Formal linearization of the system (1) with respect to the parameters of the medium containing terms of the first order of smallness and using expansions (5) and (6) lead to the following initial-boundary value problem for describing the wave process:

- for defining the wavefield in the background medium $(\vec{u}_0, \vec{\tau}_0)$ with the smoothly changing parameters λ_0, μ_0, ρ_0

$$(7) \quad \begin{cases} \rho_0 \frac{\partial u_x^0}{\partial t} = \frac{\partial \tau_{xx}^0}{\partial x} + \frac{\partial \tau_{xz}^0}{\partial z} \\ \rho_0 \frac{\partial u_z^0}{\partial t} = \frac{\partial \tau_{xz}^0}{\partial x} + \frac{\partial \tau_{zz}^0}{\partial z} \\ \frac{\partial \tau_{xx}^0}{\partial t} = (\lambda_0 + 2\mu_0) \frac{\partial u_x^0}{\partial x} + \lambda_0 \frac{\partial u_z^0}{\partial z} + F_{xx} \\ \frac{\partial \tau_{zz}^0}{\partial t} = (\lambda_0 + 2\mu_0) \frac{\partial u_z^0}{\partial z} + \lambda_0 \frac{\partial u_x^0}{\partial x} + F_{zz} \\ \frac{\partial \tau_{xz}^0}{\partial t} = \mu_0 \left(\frac{\partial u_x^0}{\partial z} + \frac{\partial u_z^0}{\partial x} \right) + F_{xz} \end{cases}$$

- for defining the scattered wavefield $(\vec{u}_1, \vec{\tau}_1)$ using the already found values $(\vec{u}_0, \vec{\tau}_0)$ as the right-hand sides of equations

$$(8) \quad \begin{cases} \rho_0 \frac{\partial u_x^1}{\partial t} + \rho_1 \frac{\partial u_x^0}{\partial t} = \frac{\partial \tau_{xx}^1}{\partial x} + \frac{\partial \tau_{xz}^1}{\partial z} \\ \rho_0 \frac{\partial u_z^1}{\partial t} + \rho_1 \frac{\partial u_z^0}{\partial t} = \frac{\partial \tau_{xz}^1}{\partial x} + \frac{\partial \tau_{zz}^1}{\partial z} \\ \frac{\partial \tau_{xx}^1}{\partial t} = (\lambda_0 + 2\mu_0) \frac{\partial u_x^1}{\partial x} + \lambda_0 \frac{\partial u_z^1}{\partial z} + (\lambda_1 + 2\mu_1) \frac{\partial u_x^0}{\partial x} + \lambda_1 \frac{\partial u_z^0}{\partial z} \\ \frac{\partial \tau_{zz}^1}{\partial t} = (\lambda_0 + 2\mu_0) \frac{\partial u_z^1}{\partial z} + \lambda_0 \frac{\partial u_x^1}{\partial x} + (\lambda_1 + 2\mu_1) \frac{\partial u_z^0}{\partial z} + \lambda_1 \frac{\partial u_x^0}{\partial x} \\ \frac{\partial \tau_{xz}^1}{\partial t} = \mu_0 \left(\frac{\partial u_x^1}{\partial z} + \frac{\partial u_z^1}{\partial x} \right) + \mu_1 \left(\frac{\partial u_x^0}{\partial z} + \frac{\partial u_z^0}{\partial x} \right) \end{cases}$$

In equations (8), “secondary sources” in right-hand have their supports in the places where perturbations λ_1, μ_1, ρ_1 are not equal to zero. Moreover, their amplitudes are proportional to perturbations of the medium. Excitation of these sources coincides with arrival of the incident wave. Thus, clusters of small scale irregularities are secondary sources emitting scattered waves. For clarity, we present in Fig. 1 the wavefield for three scatters located in a smooth medium.

As was mentioned above, we reformulate the problem of localization of small-scale inhomogeneities within a geological medium for the problem of finding the position of secondary sources of scattered waves generated by these inhomogeneities. To do this we use the TRM taking into account only the scattered component of the recorded wavefield.

The TRM algorithm consists of two steps. Suppose first that we have a wave field registered by a group of receivers on the free surface, emitted by some seismic source inside the medium. Then we use the time-reversed seismograms as a set

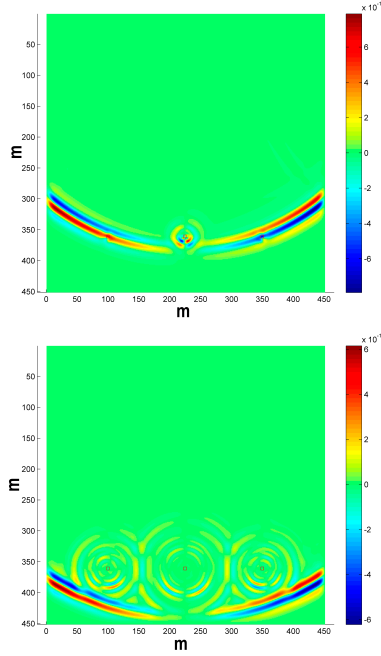


FIGURE 1. Snapshots of the wavefield component u_x for a homogeneous medium with three scatterers (red squares). (a) The wave from the source reaches scatterers (upper figure). PP and PS scattered waves generated by the local inhomogeneities (lower figure).

of sources (at the same locations as the receivers) to generate waves propagating in reverse time. Those waves should theoretically be focused synchronously into source position.

To improve the resolution of small-scale inhomogeneities, we use special techniques. The TRM procedure is sequentially applied for a set of sources uniformly distributed over a horizontal line on the free surface, followed by summing up the results obtained for each source. In addition, to eliminate the local extrema of the wave fields and to enhance the coherent component of the total wave field, we stack the elastic energy density on each time step [10]. This means that at each computational moment of time t^k for all points of computational domain, the total energy density E for all previous time steps t^m is calculated:

$$(9) \quad E_{sum}(x_i, z_j, t^k) = \sum_{t^m \leq t^k} E(x_i, z_j, t^m)$$

where elastic energy density at the time t^m computed by the following relations:

$$(10) \quad E(x_i, z_j, t^m) = \tau_{xx}(x_i, z_j, t^m)\varepsilon_{xx}(x_i, z_j, t^m) + \\ + \tau_{zz}(x_i, z_j, t^m)\varepsilon_{zz}(x_i, z_j, t^m) + 2\tau_{xz}(x_i, z_j, t^m)\varepsilon_{xz}(x_i, z_j, t^m)$$

Here τ and ε are the stress and the strain components, respectively.

In the next section we present the results of numerical experiments to demonstrate how TRM works for scatterers localization.

4. NUMERICAL SIMULATIONS

To test the proposed approach let us start with the problem of restoring the position of random small-scale inclusions in a smooth elastic medium (Fig. 2a). To do this, we assume that a smooth reference medium ($v_p = 3000$ m/s, $v_s = v_p/\sqrt{3}$, $\rho = 2000$ kg/m³) fills the square 1500×1500 m and use the finite difference staggered grid with step of 1 m. Scattering objects are introduced into this model according to the following rule:

- The entire layer is divided into rectangles of 30 m wide. (Fig. 2b);
- The presence/absence of a small-scale inclusion (scatterer) at the center of each rectangle is determined by a test of some random variable;
- If the test is successful, a square object of 3×3 m is placed at the center of the rectangle; the velocity in this object (both, compressional and shear) vary by 10% (up or down) from the velocity in the homogeneous medium.

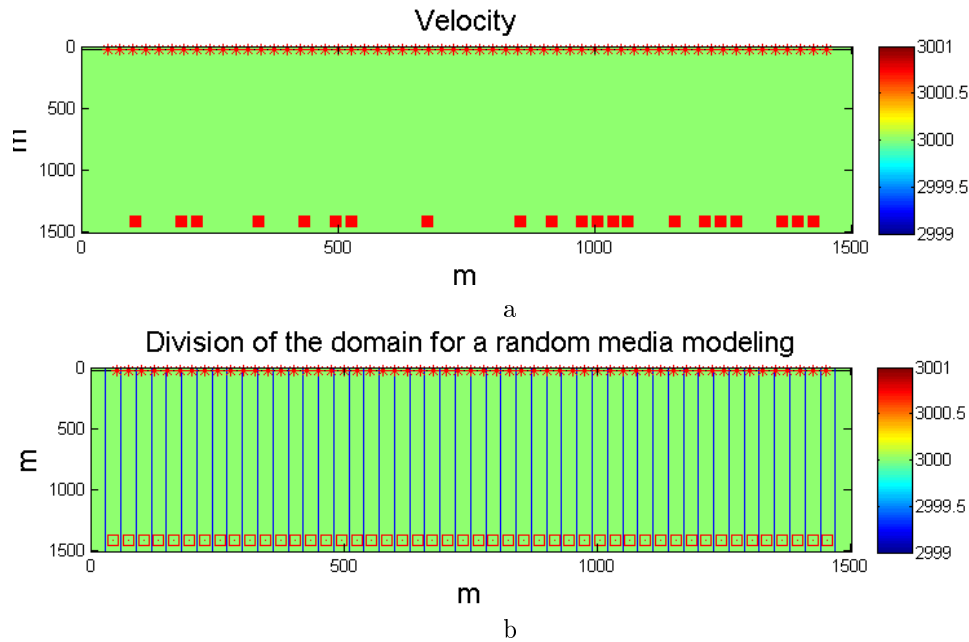


FIGURE 2. (a) The line R location of sources/receivers (red *) and random small-scale inclusions (red squares); (b) The scheme of a random media modeling.

To conduct the experiment, we need seismogram. As we have not any field data, we use synthetic seismic data obtained by numerical simulation by the staggered-grid finite difference technique with second order of accuracy with respect to space and time [8, 11]. This is a highly efficient and concise approach to simulate seismic wavefields because it directly takes into consideration the structure of the equations that form a hyperbolic system.

In this study, we do not take into account the presence of a free surface. We assume that seismograms are recorded in a horizontal line inside the unlimited space. For this purpose, the entire computational domain is surrounded by the

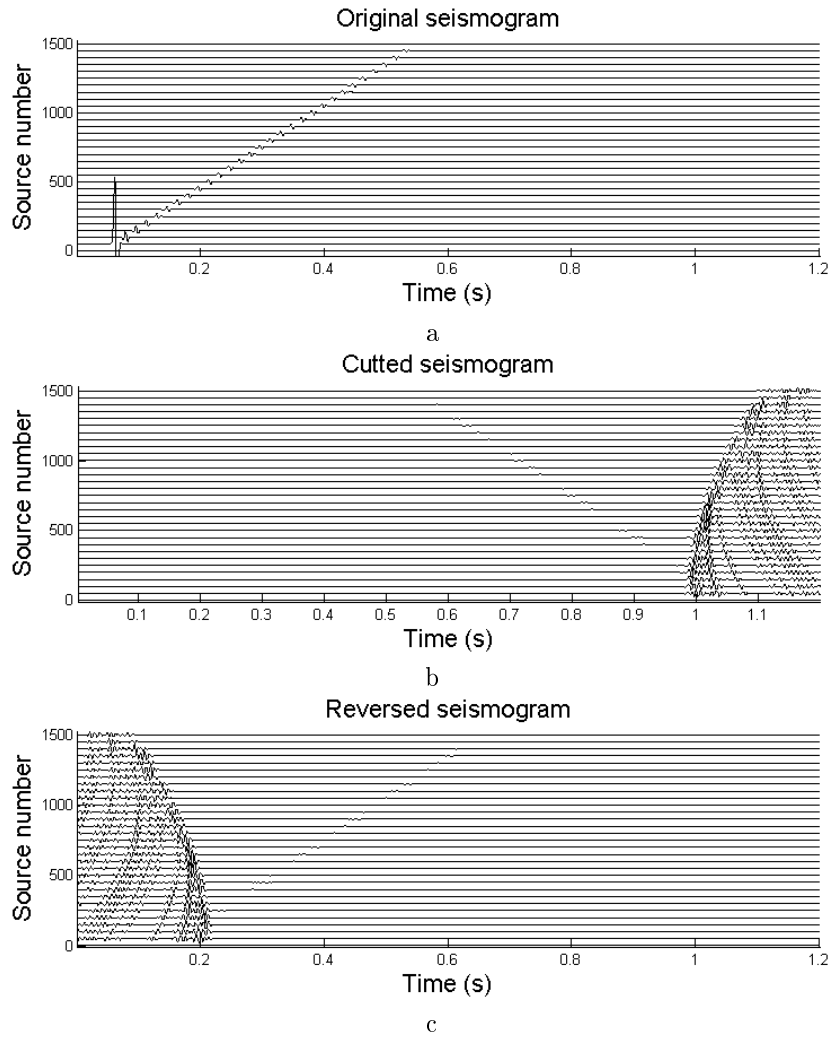


FIGURE 3. Seismogram of component τ_{zz} calculated for the first source. (a) The original seismogram; (b) Cutting off part of the seismogram from 0 to 0.8 s corresponding to the direct wave from the source and leaving a scattered wavefield part from 1 s to 1.2 s; (c) The final time-reversed seismogram using as input data for TRM procedure.

Convolutional Perfectly Matched absorbing boundary Layers (CPML) to suppress all non-physical reflections from the boundaries of the computational domain [7]. The solution of system (1) is computed up to the time $T = 1.2$ s with a time sampling step of $2 \cdot 10^{-4}$ s. To simulate the full range synthetic seismic data we used 57 sources of volumetric type (see the observation system R in Fig. 2a) located at a depth of 40 m with 2 m distance from each other. The dominant frequency of source functions is $f_0 = 100$ Hz.

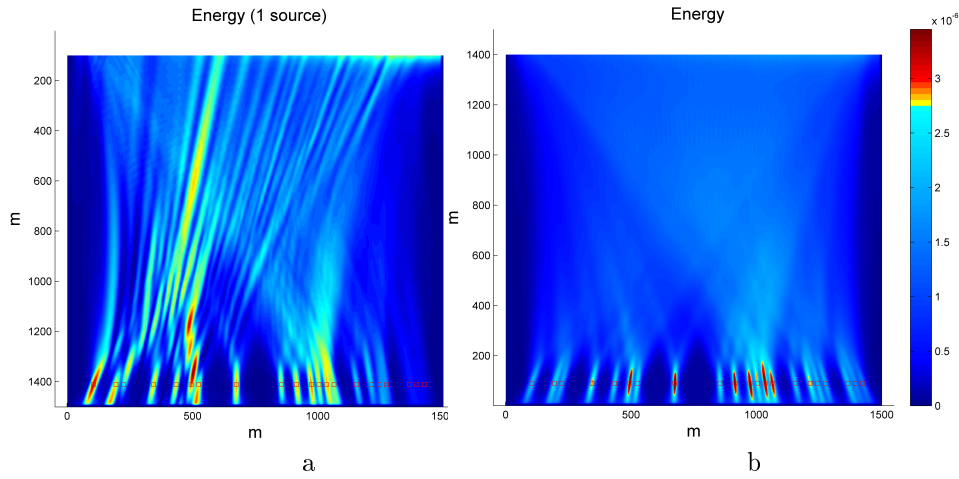


FIGURE 4. (a) A snapshot of the total energy density E calculated only for the first source; (b) A snapshot of the total energy density E sum calculated for all 57 sources.

For each position of the source, the values of the stress components (τ_{xx}, τ_{zz}) at each instant of the time are recorded in a row of receivers R (Fig. 2a) located on the free surface. The calculated seismograms are used as synthetic data for the TRM procedure.

As is known, a seismogram contains complete information about the propagation of a wavefield, including incident, reflected, transmitted, refracted, and scattered waves. The amplitude of the scattered waves is an order of magnitude smaller than the amplitude of the wave excited by the source. To increase the resolution, we cut out a part of the seismogram, leaving only the part that carries information about the scattered component of the wave field (Fig. 3). The cut of seismograms are inverted in time and considered as the initial data for the TRM inversion. In accordance with the TRM procedure described above, each seismogram acts as a set of sources generating a wavefield propagating in the medium backward in time.

The result of computations are presented in Fig. 4, where Fig. 4a shows a snapshot of the total energy density E calculated only for the first source and Fig. 4b shows the total energy density E summed at each time step for all 57 sources and recorded as snapshot at each point of the computational domain. We can observe a good correlation between the position of the scatterers in Fig. 2a and the expansion of amplitudes in Fig. 4b. Note that scatterers closer to the center of the domain recover better than scatterers at the edges. This is due to the observation system and the lack of information for the reconstruction of scatterers at the edges of the domain.

For the next test calculation, we chose the same homogeneous background but another rule for determining random scatterers. The scatterers are replaced by a random cluttered layer 100 meters thick below 1400 m with correlation length 15 m and standard deviation 5 % (Fig. 5).

For comparison, Fig. 6a shows the initial velocity distributions of the cluttered layer, and Fig. 6b shows the result of the TRM image of the total energy density E

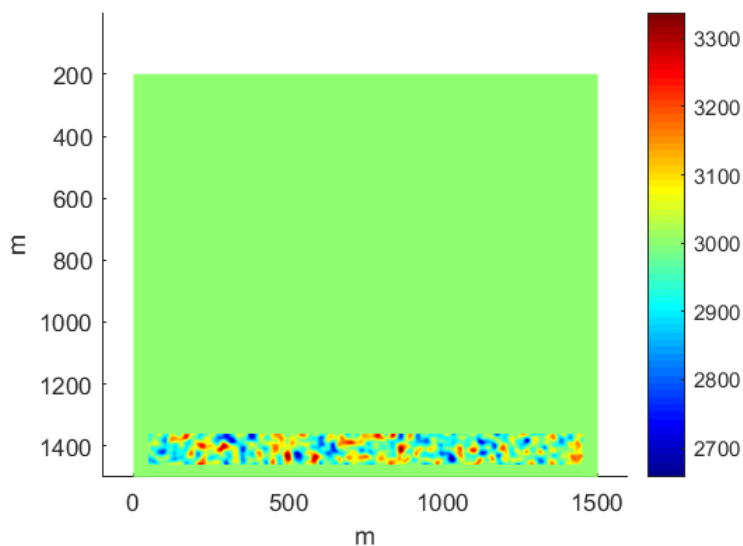


FIGURE 5. V_p velocity model for homogeneous medium with a cluttered layer.

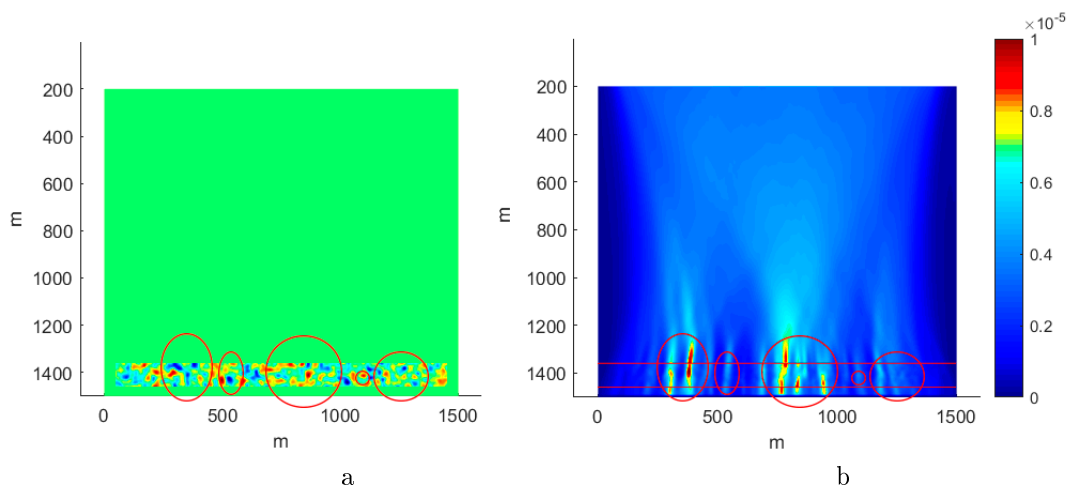


FIGURE 6. (a) The initial V_p velocity for the cluttered media; (b) A snapshot of the total energy density E summed for all sources.

summed for all sources. In this test, we also see a good match between the velocity inhomogeneities correspond to the cluttered medium in Fig. 6a and the amplitude expansion in Fig. 6b.

5. CONCLUSION

The paper presents a method for reconstructing subsurface scattering objects based on the combination of the Time Reversal Mirror with imaging of their locations by the total energy density E .

It is proved that the localization of small-scale inhomogeneities in space can be replaced by the procedure for restoring the position of the sources of scattered waves excited in the medium during seismic exploration. Numerical calculations for test models showed a good spatial reconstruction of scatterers.

Calculations have shown that for lateral resolution it is necessary to take a large observation aperture.

ACKNOWLEDGEMENTS

This work was financially supported by the Russian Science Foundation, grant No. 22-21-00759, <https://rscf.ru/en/project/22-21-00759/>.

The research is carried out using the equipment of the shared research facilities of HPC computing resources at the Siberian Supercomputer Center [13].

REFERENCES

- [1] D. Givoli., *Time reversal as a computational tool in acoustics and elastodynamics*, J. Comput. Acoust., **22**:3 (2014), Article ID 1430001. Zbl 1360.76001
- [2] M. Fink, F. Wu, D. Cassereau, R. Mallart, *Imaging through inhomogeneous media using time reversal mirrors*, in *Sixteenth International Symposium on Ultrasonic Imaging and Tissue Characterization, June 3-6 1991, Arlington, VA*, Ultrasonic Imaging, **13**:2 (1991), 199.
- [3] M. Fink, *Time reversal in acoustics*, Contemp. Phys., **37**:2 (1996), 95–109.
- [4] M. Fink, *Time reversed acoustics*, Phys. Today, **50**:3 (1997), 34–40.
- [5] M. Fink, G. Montaldo, M. Tanter, *Time-reversal acoustics in biomedical engineering*, Annu. Rev. Biomed. Eng., **5** (2003), 465–497.
- [6] M. Fink, C. Prada, *Acoustic time-reversal mirrors*, Inv. Probl., **17**:1 (2001), R1–R38. Zbl 0974.35131
- [7] D. Komatitsch, R. Martin, *An unsplit convolutional perfectly matched layer improved at grazing incidence for the seismic wave equation*, Geophysics **72**:5 (2007), sm155–sm167.
- [8] A.R. Levander, *Fourth-order finite-difference P-SV seismograms*, Geophysics **53**:11 (1988), 1425–1436.
- [9] M. Protasov, G. Reshetova, V. Tcheverda, *Fracture detection by Gaussian beam imaging of seismic data and image spectrum analysis*, Geophysical Prospecting **64**:1 (2016), 68–82.
- [10] G.V. Reshetova, A.V. Anchugov, *Digital core: simulation of acoustic emission in order to localize its sources by the method of wave field reversal in reverse time*, Geology and geophysics, **62**:4 (2021), 597–609.
- [11] J. Virieux, *P-SV wave propagation in heterogeneous media: Velocity-stress finite-difference method*, Geophysics **51**:4 (1986), 889–901.
- [12] K. Wapenaar, J. Thorbecke, *Review paper: Virtual sources and their responses, Part I: Time-reversal acoustics and seismic interferometry*, Geophysical Prospecting **65**:6 (2017), 1411–1429.
- [13] Novosibirsk Supercomputer Center of SB RAS, <http://www.sccc.icmmg.nsc.ru>

GALINA VITALIEVNA RESHETOVA
 INSTITUTE OF COMPUTATIONAL MATHEMATICS AND MATHEMATICAL GEOPHYSICS SB RAS
 6, ACAD. LAVRENTIEVA AVE.,
 NOVOSIBIRSK, 630090, RUSSIA
 Email address: kgv@nmsf.sccc.ru

ANASTASIA ANDREEVNA GALAKTIONOVA
INSTITUTE OF COMPUTATIONAL MATHEMATICS AND MATHEMATICAL GEOPHYSICS SB RAS
6, ACAD. LAVRENTIEVA AVE.,
NOVOSIBIRSK, 630090, RUSSIA
Email address: galakt95@mail.ru